Chapter 14
Measuring and Modelling Soil Depth Functions

Budiman Minasny, Uta Stockmann, Alfred E. Hartemink and Alex B. McBratney

Abstract Hans Jenny stated that the anisotropy of soil with depth means that the soil has a unique profile. Therefore, naturally every soil property has its specific depth function. The changes of soil particle size distribution in a soil profile can be used as an indicator of soil formation and processes and has been used as a proxy for soil age or degree of development. Uniform, gradational and rapidly changing (duplex) soil textures are examples of soil profile forms used for soil classification in Australia. Various parametric and nonparametric depth functions have been used to describe the variation of soil properties with depth. We have identified 7 typologies of depth functions: uniform, gradational, exponential, wetting front, abrupt, peak and minima–maxima. These depth functions are related to soil-forming processes. To test these functions, a proximal soil sensor was used to perform in situ digital morphometrics by which soil properties are measured along a soil profile wall at small depth increments. We explore the possibility of horizon boundary detection based on the changes in elemental concentrations. It was concluded that digital morphometrics enables soil scientists to measure the soil's depth functions and weathering history quantitatively directly in the soil pit and assists in more objective delineation of soil horizons.

Keywords In situ pXRF analysis · Soil depth functions · Weathering indices · Soil profile development · Soil horizons

B. Minasny (✉) · U. Stockmann · A.B. McBratney
Faculty of Agriculture and Environment, The University of Sydney, New South Wales 2006, Australia
e-mail: budiman.minasny@sydney.edu.au

A.E. Hartemink
Department of Soil Science, University of Wisconsin—Madison, FD Hole Soils Lab, 1525 Observatory Drive, Madison, WI 53706, USA

A.E. Hartemink and B. Minasny (eds.), *Digital Soil Morphometrics*, Progress in Soil Science, DOI 10.1007/978-3-319-28295-4_14

14.1 Introduction

Hans Jenny (1941) noted that naturally, every soil property has its own vertical distribution pattern or specific "depth function". Most soil scientists work on data collected from soil horizons. Jenny (1941) and (Arkley 1976) stated that the assignment of horizons and their names is difficult and can be subjective. Jenny suggested the use of the soil indicatrix (a laterally isotropic 3-D depth function) for clarification and refinement of soil profile descriptions.

Measurements of soil properties in a soil profile are usually made based on the horizons, or defined depth intervals. Samples or measurements are usually bulked based on the horizons, resulting in "stepped" data which may mask the continuity of soil properties (Hartemink and Minasny 2014). Soil scientists also measure soil properties at fixed depth intervals (e.g. every 10 cm) to reveal the depth functions of certain soil physical and chemical properties [e.g. (Walker and Green 1976)]. For example, soil organic carbon and total nitrogen, representing biotic components, commonly decrease exponentially with depth, whereas clay and iron, representing mineral components, can be low in the A horizon and highest in the B horizon. Colwell (1970) noted that most chemical properties show continuous trends throughout the soil profile. Depth function characterisation of soil properties is thus needed to show profile trends in addition to particular horizons.

This paper first reviews soil depth functions found in the literature, from pedological observations, to mechanistic models. We then suggest some common soil depth function typologies and reason how they relate to soil-forming processes. We will present examples of depth functions of soil elemental concentration measured in the field using a pXRF instrument.

14.2 A Review of Soil Depth Functions

14.2.1 Pedological Models

Northcote (1971) introduced principal soil profile forms resulting from his observations of many soil profiles in Australia. His book *Factual Key for the Recognition of Australian Soils*' first division of soil profile is based on its primary profile forms: organic, uniform, gradational and duplex. Mineral soils are distinguished by the depth trend in texture. Uniform profiles have little or no change in texture; gradational profiles show a steady increase of clay content with depth, and duplex profiles have layers of contrasting texture within the solum (Fig. 14.1). The profile forms also imply the degree of soil development from minimum development (uniform), to moderate development with some illuviation process (gradational), and pronounced development with heavy illuviation (duplex).

For young soils developed from till (Madsen and Munk 1987), as reported in Adhikari et al. (2014), the degree of soil development can be estimated from the

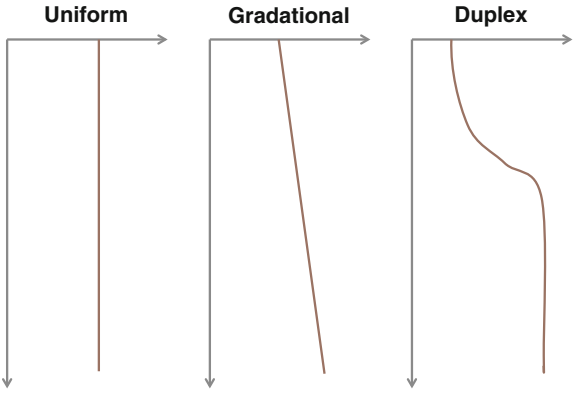

Fig. 14.1 Principal soil profile form as recognised by Northcote (1971)

trend of pH with depth. A soil after the deposition of carbonate rich parent material will have a uniform high pH and was considered young (Fig. 14.2a). With time, leaching of carbonates created a gradational (b) and duplex (c) soil pH which increased with depth. When these soils (b and c) are limed, the depth function changed towards profile (d and e), respectively (Adhikari et al. 2014).

14.2.2 Analytical Models

Kirkby (1977) proposed several depth functions which relate to the distribution of organic material, water, and evaporation and transpiration processes. The shapes of the functions included the following: exponential decay, convex and minima–maxima (Fig. 14.3). The exponential function assumes the distribution of organic

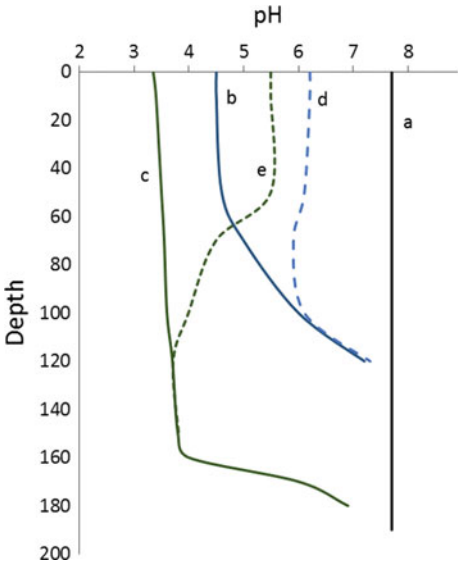

Fig. 14.2 Leaching and liming effect on soils developed in lime-rich till in Denmark. Soil profile **a** newly deposited till; **b** weakly leached soil; **c** strongly leached soil; **d** soil **b** limed; and **e** soil **b** limed (adapted from Madsen and Munk 1987)

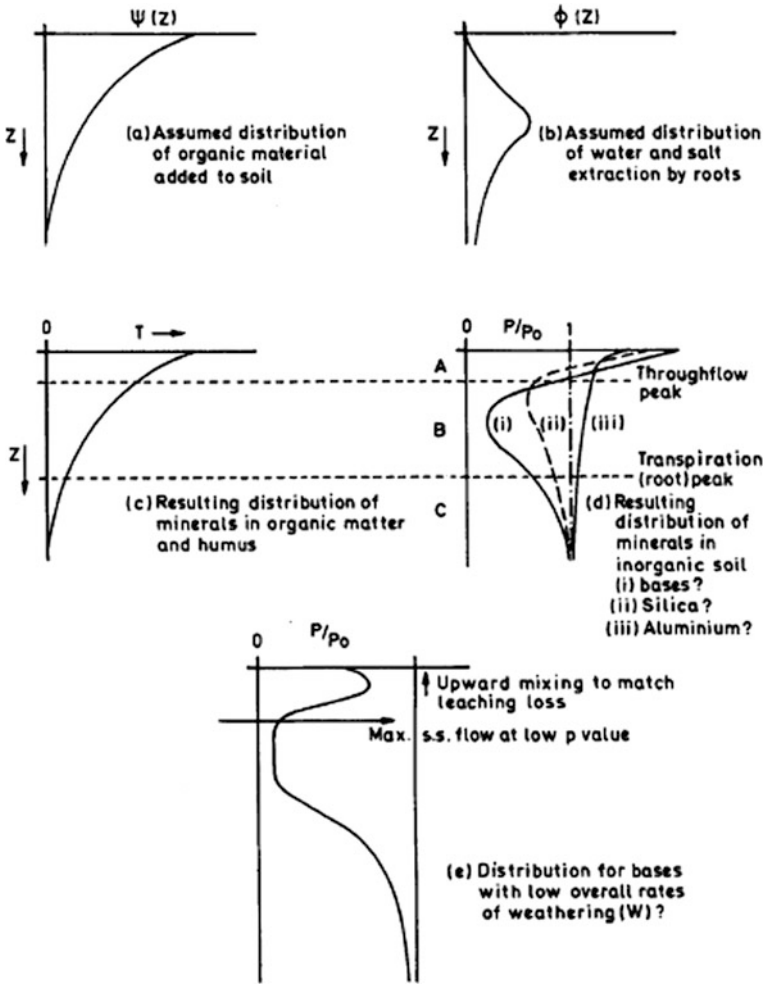

Fig. 14.3 Features of equilibrium soil profile predicted by an analytical soil profile development model [from Kirkby (1977)]

matter that was added to soil via plant litter or decaying of roots. The bell-shaped function assumes the distribution of water and the movement of solutes, and their extraction by plant roots. Mixing in the surface layer can create minimum–maximum peaks. We will discuss these functions in the next sections.

14.2.3 Exponential or Power Functions

The most widely used model for soil depth functions is the exponential or power function, which is mainly used to describe the distribution of soil organic matter or

organic carbon content with depth. The function describes the decline of soil organic matter or carbon with depth (highest in the A horizon, and low in the subsequent horizons). Russell and Moore (1968) proposed a simple exponential function:

$$C(z) = C_0 \exp(-kz)$$

where C_0 is the carbon concentration at the soil surface and k is the rate of decrease, and z is depth. They mentioned that this function is similar to the profile depth of biological properties, e.g. plant roots. This function can model a range of shapes, from a highly exponential to a linear decrease of concentration with depth. Variations of this exponential function have been proposed to describe the decrease of soil carbon with depth (Bernoux et al. 1998). A power function can also display such trend with depth (Fig. 14.4):

$$C(z) = C_0 z^b$$

The soil organic carbon content in the plough layer of cultivated fields is often relatively uniform, and a constant can be introduced for that zone as shown in Fig. 14.4b (Mikhailova et al. 2000; Meersmans et al. 2009). In spodosols, a second maxima of SOC often occurs in the spodic horizon (Webster 1978). A similar pattern also occurs in the presence of buried horizons and in palaeosols (Fig. 14.4c) (Grauer-Gray and Hartemink 2016).

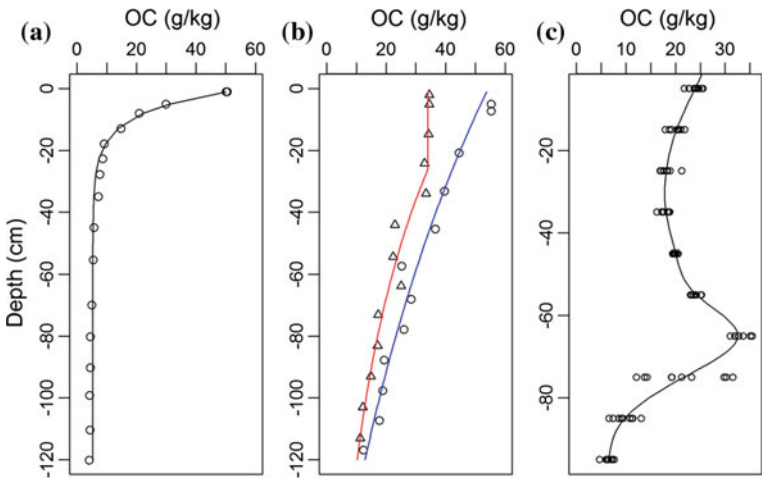

Fig. 14.4 Depth function of soil organic carbon, **a** an exponential function in an alluvial soil in New South Wales, Australia (Walker and Green 1976), **b** a grassland (*circle*) and a continuously cropped field (*triangle*) of Chernozems from Russia (Mikhailova et al. 2000), and **c** a Mollisol with a buried A horizon at 70 cm depth from South Central Wisconsin, USA (Grauer-Gray and Hartemink 2016)

The negative exponential depth function can also be used to describe soil temperature as an analytical solution to heat transport. The incorporation of organic matter through bioturbation in soil modelled as a diffusion process often results in an exponentially shaped depth function. The depth-exponential relation is also found in the soil production function, where the soil weathering rate decreases with increasing soil thickness (Stockmann et al. 2014).

14.2.4 Wetting Front

The movement of water through a soil profile creates wetting front-type depth functions. A mechanistic model by Kirkby (1985) with diffusion processes results in the weathering profile that resembles a wetting front. Brantley et al. (2008) observed that most chemical and mineralogical profiles display reaction fronts that show depletion of leachable elements or minerals (Fig. 14.5). They modelled the depth function in the form of a sigmoidal function:

$$C(z) = \frac{C_m}{1 + \frac{C_m - C_0}{C_0} \exp(\alpha\, z)}$$

where C is the concentration at depth z, with an empirical parameter α.

Beaudette et al. (2016) modelled the depth distribution of soil horizons using a proportional odds logistic regression which has a form similar to the sigmoid

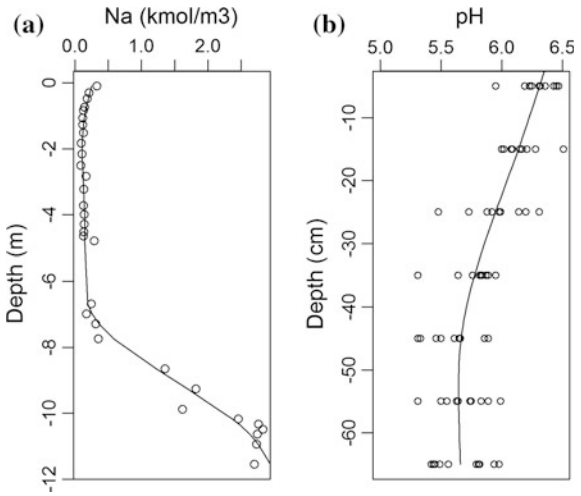

Fig. 14.5 Wetting front-type depth functions for: **a** Concentration of Na in Panola granite soil in the Piedmont Province of Georgia, USA, exposed to weathering for approximately 250–500 ka [data from Brantley et al. (2008)], **b** Soil pH from an intensely cultivated Udic Psamments from the Central Sands of Wisconsin, USA (Adhikari et al. 2016)

function. Leblanc et al. (2016) found a wetting front-type depth function for gleyed horizons, but a peak function for spodic horizons.

14.2.5 Peak Functions

Some soil properties such as clay content show accumulation (maxima) with depth as a result of eluviation and illuviation processes, in situ formation or discontinuity in soil parent materials. This accumulation can depict a bell-shaped curve, which is a characteristic of solute transport. Solute transport in soil can exhibit a normal distribution for dispersion and diffusion processes (Wetselaar 1962) or a lognormal distribution function for convective processes (Jury 1982) (Fig. 14.6). The analytical solution for a convective-diffusion transport during weathering by (Kirkby 1985) suggests a double exponential function. Myers et al. (2011) observed that some soil profiles showed highly asymmetric peak-shaped depth distributions for some soil properties. The asymmetry occurred mainly due to the gravitational vector of profile weathering and development. They proposed the use of the Pearson-type IV (PIV) asymmetric probability density function or logistic peak function. The parameters of the model can be related to properties' maximum, depth to the maximum, abruptness, and profile anisotropy. Peak functions can also indicate compaction, and anthropogenic influences can create variations such as multiple peaks (Fig. 14.7a).

An extension of the peak model is observed in properties such as clay content or electrical conductivity (Bishop et al. 1999), where its value reaches a minimum and increases to a maximum (Fig. 14.7b). This minima–maxima (minimax) depth function can be related to mixing processes in the surface and translocation to the

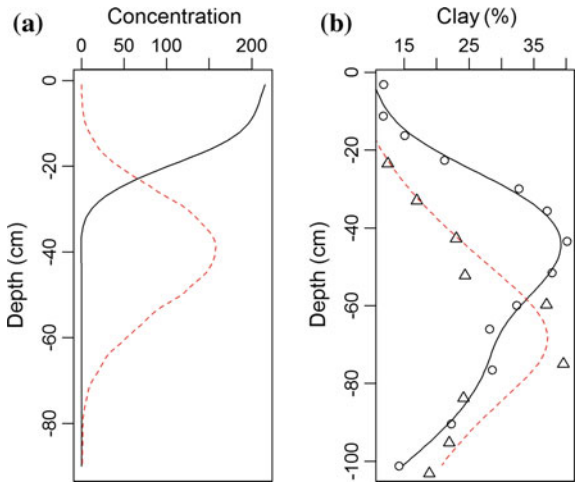

Fig. 14.6 **a** Theoretical depth distribution of solute transport in soil; solute initially follows the wetting front and displays a bell-shaped distribution following convection–dispersion processes. **b** An example of peak distribution function for clay content

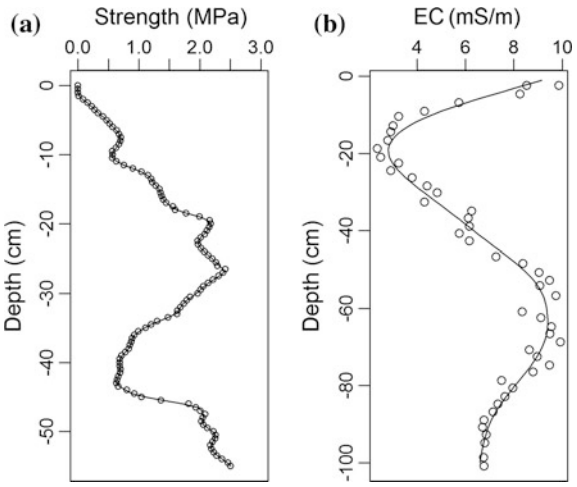

Fig. 14.7 **a** Penetration resistance from a cone penetrometer for a cultivated field showing multiple peaks [data from (Minasny 2012)], and **b** electrical conductivity from a *red* podzolic soil (Alfisol) in New South Wales, Australia, showing a minima–maxima pattern [from Bishop et al. (1999)]

subsurface, through excessive bioturbation, or textural discontinuities resulting from different parent materials within the soil profile.

14.2.6 Abrupt or Lithologic Discontinuity

Abrupt changes in the soil properties in the profile can be due to changes in the lithology of soil parent materials (Schaetzl 1998). When they occur within or near the solum, they can impact pedogenesis. Sudden increase in coarse sand or layers of gravel are common indicators of lithologic discontinuity. In environments with sharp discontinuities due to deposition or human influences, the depth functions of soil properties change abruptly. Kempen et al. (2011) modelled the depth functions for soil organic carbon of soils that have composite or stacking of discontinued horizons, where each horizon has either a linear or an exponential function. This resulted in discontinuous depth functions with abrupt boundaries.

14.2.7 Polynomials and Splines

Linear regression and orthogonal polynomials of 2nd-degree to 5th-degree have been fitted to soil depth data (Colwell 1970). This allows a degree of variation within the depth, but there are disadvantages as there is no theory from which to determine a suitable degree of polynomial and local variation can affect the quality of fit elsewhere in the soil profile (Webster 1978). Erh (1972) proposed the use of splines as a flexible function that can fit a piece wise a series independent polynomial functions over small intervals of a soil profile and also produces a

continuous derivative function. Webster (1978) demonstrated that the spline interpolators are better for some organic matter profiles of soils in Britain, especially for Spodosols where the exponential decrease assumption is invalid.

Ponce-Hernandez et al. (1986) pointed out that many of the proposed methods fit the depth functions or curves through the depth of horizon averages. This can produce unreliable results as it smoothens out the variance of the data. The fitted curves can be smoother than the true variation of the properties with depth. They proposed equal-area splines to reconstruct profiles more accurately from stepped data and the approach was used by Slater (1994) to reconstruct soil horizon data into a more regular depth interval for a continuous classification. Bishop et al. (1999) proposed the equal-area quadratic smoothing splines and tests of their model indicated the superiority of equal-area splines in prediction of depth functions.

The development of proximal soil sensors allows measurements of soil properties at small depth increments with depth. Invasive, in situ technologies include penetrometer with penetration resistance measurement (Arriaga et al. 2016) which can be coupled with moisture content and bulk electrical conductivity sensors.

14.2.8 Typologies of Depth Functions

Based on the above review, we have identified common typologies of soil depth functions. The shape of the functions imply physical processes as described above. In essence, there are 7 typologies that describe soil property change with depth: uniform, gradational, exponential, wetting front, abrupt, peak, and minima–maxima (minimax) (Fig. 14.8). The curves have mirror images reflecting properties that

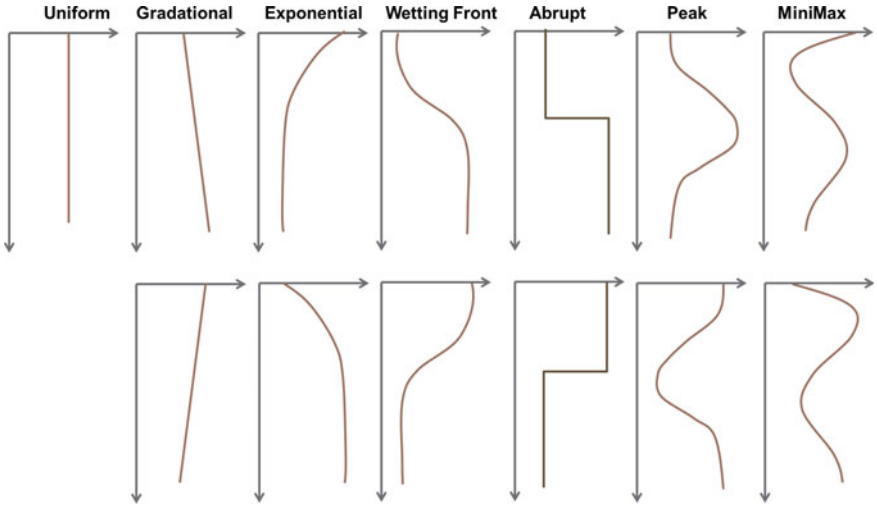

Fig. 14.8 General typologies of depth functions

might be compositional or complementary. The patterns may or may not reflect soil horizon boundaries.

14.3 Profile Development Indices

Pedologists study the depth functions to infer soil processes and development. Profile development indices were developed based on the horizons' morphological and chemical data as quantitative measures of stages of soil profile development. For example, Harden (1982) developed a soil profile development index that was related to the age of the soil. The index was calculated as a sum of field and laboratory data weighted by the horizon thickness.

Another index related to profile development is the Index of Profile Anisotropy (IPA) was developed by Walker and Green (1976) which provides a single value to describe the anisotropy of a profile with laboratory-measured soil data. When a soil is very young, its properties are assumed to be isotropic in nature (such as a uniform texture). When a soil matures and is more intensely weathered, the anisotropy value is increased. IPA is defined as follows:

$$\text{IPA} = |\text{Deviation}|/\text{mean}$$

At time = 0 soil properties are isotropic; with time, soil properties change with depth, the degree of anisotropy increases with time. The depth functions can now be used to calculate these indices as a quantitative measure the degree of soil profile development.

14.4 Soil Depth Function Examples

To demonstrate the idea of depth functions, we show the measurement of elemental concentration of soils in the field. Measurements were made every 5 cm along the profile wall of an Alfisol and an Entisol in Wisconsin, USA, using an Olympus pXRF operated in GEOCHEM mode.

14.4.1 Mollic Hapludalfs

The Mollic Hapludalfs from West Madison has developed in loess over coarse and calcareous outwash and the soil has 5 soil horizons. The plough layer is 24 cm deep with a silt loam followed by a silty clay loam Bt horizon (24–55 cm). There is a transitional BC horizon (55–91 cm) adjacent to the outwash (horizon 2 C) where the texture is a loamy sand. Figure 14.8 shows depth functions of some major elements measured in the soil pit. The Al and Fe concentrations show a similar pattern with a peak in the Bt horizon, indicating that there is enrichment with

alumino-silicates—an indication of clay illuviation. The Mn concentration varies gradually down the profile with an increase in the Bt horizon. There is a colour and morphology change from the Ap to the Bt horizon, but most elements measured by pXRF varies smoothly down the profile.

Elemental concentration from pXRF allows calculation of soil chemical weathering indices that were developed for pedological studies (Sauer et al. 2007). The main assumption of these indices is that the concentration and movement of chemical elements are controlled by the degree of weathering. It is assumed that during the weathering process, major oxides such as TiO_2 and Fe_2O_3 and Al_2O_3 are considered immobile, and Si_2O, K_2O, Na_2O, MgO and CaO are mobile. Most of these weathering indices are expressed as a ratio of molecular or weight percentage between different elements or groups of major oxides (Sauer et al. 2007). The simplest weathering index is SiO_2/Al_2O_3 (Ruxton 1968) which captures the loss of silica during weathering. It is assumed that the amount of alumina in weathered soil is immobile and constant and the amount of oxides (zirconia, titanium and total iron oxides) is constant. The index ranges from a high value (around 10 for unweathered material) to a low for weathered soil. It is mostly used for studying highly weathered soils. Another index is the Ti/Zr ratio, and these immobile elements are highly correlated and have been used to test the homogeneity of parent materials (Maynard 1992). The Ti/Zr ratio is not much affected by primary alteration or weathering and can be used as indicator of major igneous rock types.

We calculated these two weathering indices for the Alfisol (Fig. 14.9). Although the 2C horizon is a parent material discontinuity (starting at 60 cm), most elements did not reflect this abrupt change except for elemental Ca concentrations. The Zr concentration shows a wetting front-type depth function with a constant value to a depth of 50 cm and gradually decreasing at 80 cm depth where the Zr concentrations are low. The Ti/Zr ratio shows a convex or peak function with a spike at the horizon boundary at 90 cm depth. The SiO_2/Al_2O_3 ratio is low and around 5 up to 80 cm soil depth and increases from 8 to 14 to a depth of 150 cm. The elemental concentration that mostly shows a smooth variation across the 2 parent materials indicates that there has been mixture through diffusion process.

14.4.2 Typic Udipsamments

The Typic Udipsamments from the Wisconsin central sand plain is characterised by a blanket of sandy and gravelly outwash. The soil is the plainfield sand series consists of very deep excessively drained soils formed in sandy drift on outwash plain, glacial lake basins, stream terraces, and moraines.

The profile has an Ap horizon of 24 cm which is reflected in the variation of Fe and Mn. The depth function of Fe shows a constant value for the Ap horizon followed by a peak at 60 cm. The depth function of P follows an exponential form, decreases with depth, with P sourced from inorganic fertiliser input. The Al and Si concentrations show a bowl-shaped depth function indicating some mixture of

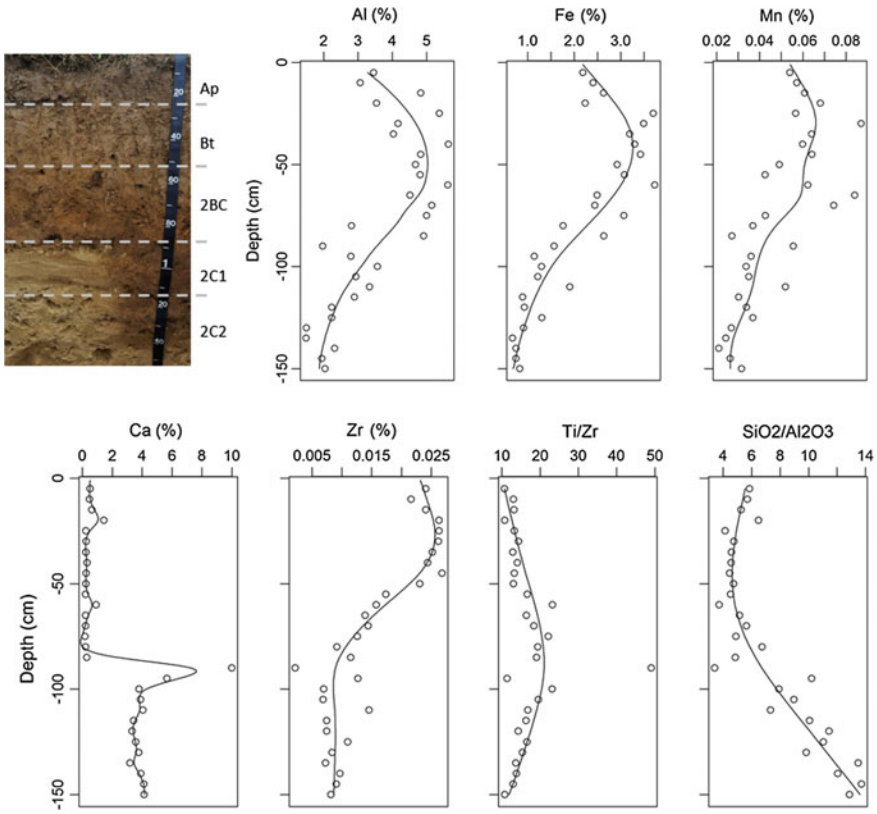

Fig. 14.9 Depth functions of a Mollic Hapludalfs from West Madison, Wisconsin, USA. Concentration of Al, Fe, Ca, Zr, Ti/Zr and SiO_2/Al_2O_3 was measured using a pXRF in the field at 5-cm-depth intervals along the soil profile wall. The lines are fitted smoothing splines

materials in the Ap horizon, leaching of materials in the Bw1 and Bw2 horizons and unweathered materials in Bw3. This pattern is reflected in the SiO_2/Al_2O_3 ratio, where the pattern is a reverse of a weathered soil profile (increasing weathering down the profile). The index reflects leaching of Si, and the assumption of Al as constant is invalidated. The Ruxton index may not be suitable for this soil as an indication of weathering. The Ti/Zr ratio is uniform throughout the profile with an increasing value in the Bw3 horizon indicating less weathered soil materials (Fig. 14.10).

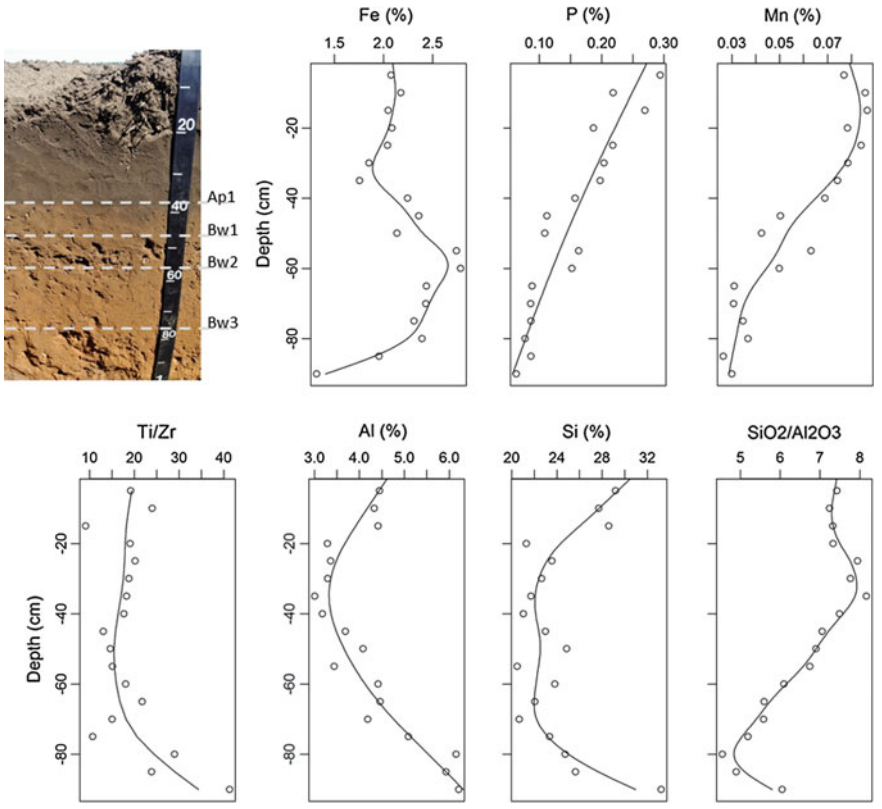

Fig. 14.10 Depth functions of a Typic Udipsamments from the Central Sands, Wisconsin, USA. Concentration of Fe, P, Mn, Ti/Zr, Si, Al and SiO_2/Al_2O_3 was measured using a pXRF at 5-cm-depth intervals along a soil profile wall. The lines are fitted smoothing splines

14.4.3 Horizon Boundary Detection Using Soil Depth Function Data

The depth functions of the elements are mostly continuous as opposed to the discrete appearance and assumptions in soil horizons. We can use pedometric techniques to segment these into layers and reconcile the layers with field observed horizons (Weindorf et al. 2012). The depth functions can be treated as transect with multivariate measurements of elemental concentration. The horizon boundaries can be identified based on the Mahalanobis distance of a split moving window approach of (Webster 1973) or the difference between subsequent pXRF readings as proposed by (Weindorf et al. 2012). We can also apply a fuzzy k-means clustering of the elemental concentration to create soil material classes (Fajardo et al. 2015). In this example, fuzzy k-means clustering was applied to identify layers of similar characteristics within each profile. In our example (Fig. 14.11), both profiles were

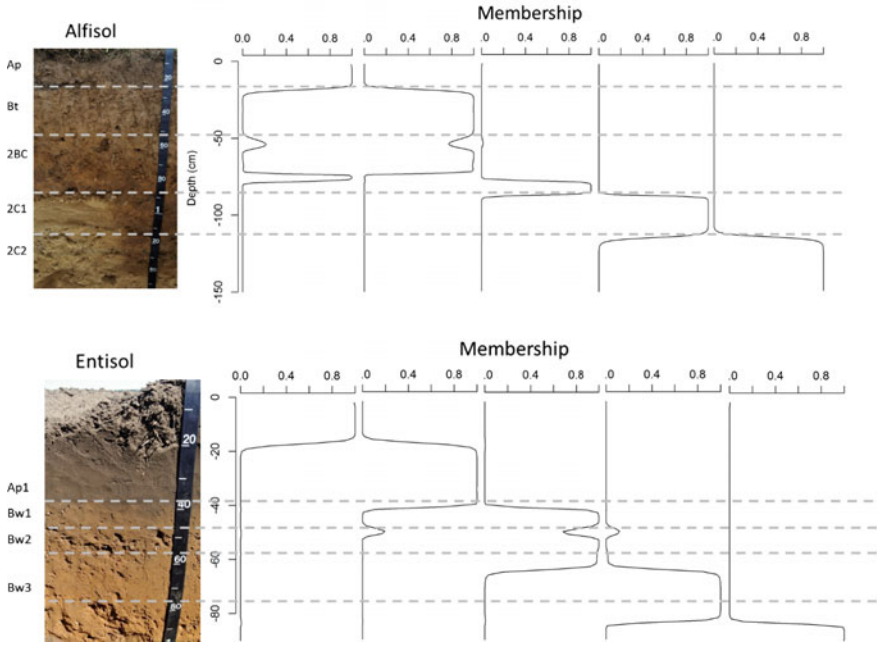

Fig. 14.11 Elemental concentration data (Fe, Mn, Al, Ca, Si) for each profile were grouped using a fuzzy k-means clustering method. The data for each profile were clustered into 5 classes individually, and the plot shows the membership for each of the class

grouped individually into 5 classes based on their elemental concentration. The membership for each class occupied a unique layer within the profile, and some of the numerical classes correspond to the horizons observed in the field. For example in the Alfisol, the numerical class corresponds to the Ap, (Bt + BC), BC, 2C1 and 2 C2. Whereas in the Entisol, the Ap horizon is separated into 2 classes.

14.5 Conclusions

We identified 7 typologies of soil depth functions: uniform, gradational, exponential, wetting front, abrupt, peak/convex and minima–maxima. These depth functions represent major soil processes. Field measurements using tools such as pXRF and NIR allow measurement of soil properties and elemental concentration at small depth increments and thus enable estimation of depth functions readily and rapidly without the need to collect bulk soil samples from horizons. The examples presented here showed that most soil elemental concentration vary continuously with depth. Although the data are few, the depth functions reflect the age of the soil, some major soil processes, parent materials, and soil textural changes. Horizon

boundaries based on elemental concentration can be derived using, for example, moving window Mahalanobis distance or fuzzy k-means clustering. Proximal soil sensors allow measurement of soil development indices in the field, which has the potential for a more objective delineation of soil horizons and description of the soil profile. A more objective measurement of the soil properties can lead to a better understanding of soil processes and within soil horizon variation.

References

Adhikari K, Hartemink AE, Minasny B (2016) Mapping a profile wall of a typic Udipsamments from the Central Sands, WI, USA. In: Hartemink AE, Minasny B (eds) Digital soil morphometrics. Springer, Dordrecht

Adhikari K, Kheir RB, Greve M, Greve MH, Malone MB, Minasny B, McBratney A (2014) Mapping soil pH and bulk density at multiple soil depths in Denmark. In: Arrouays D, McKenzie N, Hempel J, de Forges AR, McBratney AB (eds) GlobalSoilMap: basis of the global spatial soil information system. Taylor & Francis, London, pp 155–160

Arkley RJ (1976) Statistical methods in soil classification research. Advances in Agronomy. Academic Press, New York, NY, pp 37–69

Arriaga FJ, Lowery B, Reinert D, McSweeney K (2016) Cone penetrometers as a tool for distinguishing soil profiles and mapping soil erosion. In: Hartemink AE, Minasny B (eds), Digital soil morphometrics. Springer, Dordrecht, p. (this volume)

Beaudette DE, Roudier P, Skovlin J (2016) Probabilistic representation of genetic soil horizons. In: Hartemink AE, Minasny B (eds), Digital soil morphometrics. Springer, Dordrecht, p. (this volume)

Bernoux M, Arrouays D, Cerri CC, Bourennane H (1998) Modeling vertical distribution of carbon in oxisols of the Western Brazilian Amazon (Rondonia). Soil Sci 163:941–951

Bishop TFA, McBratney AB, Laslett GM (1999) Modeling soil attribute depth functions with equal-area quadratic smoothing splines. Geoderma 91:27–45

Brantley SL, Bandstra J, Moore J, White AF (2008) Modelling chemical depletion profiles in regolith. Geoderma 145:494–504

Colwell J (1970) A statistical-chemical characterization of four great soil groups in southern New South Wales based on orthogonal polynomials. Soil Res 8:221–238

Erh K (1972) Application of the spline function to soil science. Soil Sci 114:333–338

Fajardo M, McBratney A, Whelan B (2015) Fuzzy clustering of Vis–NIR spectra for the objective recognition of soil morphological horizons in soil profiles. Geoderma

Grauer-Gray JR, Hartemink AE (2016) Variation of soil properties in a Mollisol profile wall. In: Hartemink AE, Minasny B (eds) digital soil morphometrics. Springer, Dordrecht

Harden JW (1982) A quantitative index of soil development from field descriptions: Examples from a chronosequence in central California. Geoderma 28(1):1–28

Hartemink AE, Minasny B (2014) Towards digital soil morphometrics. Geoderma 230:305–317

Jenny H (1941) Factors of soil formation. A system of quantitative pedology. McGraw-Hill, New York

Jury WA (1982) Simulation of solute transport using a transfer function model. Water Resour Res 18:363–368

Kempen B, Brus DJ, Stoorvogel JJ (2011) Three-dimensional mapping of soil organic matter content using soil type-specific depth functions. Geoderma 162:107–123

Kirkby M (1977) Soil development models as a component of slope models. Earth Surf Process 2:203–230

Kirkby MJ (1985) A basis for soil profile modelling in a geomorphic context. J Soil Sci 36:97–121

Leblanc MA., Gagné G, Parent LE (2016) Numerical clustering of soil series using profile morphological attributes for potato. In: Hartemink AE, Minasny B (eds) Digital soil morphometrics. Springer, Dordrecht, p. (this volume)
Madsen HB, Munk I (1987) The influence of texture, soil depth and geology on pH in farmland soils: a case study from southern Denmark. Acta Agricul Scand 37:407–418
Maynard J (1992) Chemistry of modern soils as a guide to interpreting Precambrian paleosols. J Geol 279–289
Meersmans J, van Wesemael B, De Ridder F, Van Molle M (2009) Modelling the three-dimensional spatial distribution of soil organic carbon (SOC) at the regional scale (Flanders, Belgium). Geoderma 152:43–52
Mikhailova E, Bryant R, Vassenev I, Schwager S, Post C (2000) Cultivation effects on soil carbon and nitrogen contents at depth in the Russian Chernozem. Soil Sci Soc Am J 64:738–745
Minasny B (2012) Contrasting soil penetration resistance values acquired from dynamic and motor-operated penetrometers. Geoderma 177–178:57–62
Myers DB, Kitchen NR, Sudduth KA, Miles RJ, Sadler EJ, Grunwald S (2011) Peak functions for modeling high resolution soil profile data. Geoderma 166:74–83
Northcote K (1971) A factual key for the recognition of Australian soils. CSIRO/Rellim, Glenside, South Australia
Ponce-Hernandez R, Marriott FHC, Beckett PHT (1986) An improved method for reconstructing a soil profile from analyses of a small number of samples. J Soil Sci 37:455–467
Russell J, Moore A (1968) Comparison of different depth weightings in the numerical analysis of anisotropic soil profile data. Transactions of the 9th International Congress of Soil Science, pp. 205–213
Ruxton BP (1968) Measures of the degree of chemical weathering of rocks. J Geol 518–527
Sauer D, Schellmann G, Stahr K (2007) A soil chronosequence in the semi-arid environment of Patagonia (Argentina). Catena 71:382–393
Schaetzl RJ (1998) Lithologic discontinuities in some soils on drumlins: theory, detection, and application. Soil Sci 163:570–590
Slater BK (1994) Continuous Classification and visualization of soil layers: a soil-landscape model of Pleasant Valley Wisconsin. University of Wisconsin, Department of Soil Science, Madison, Wisconsin
Stockmann U, Minasny B, McBratney AB (2014) How fast does soil grow? Geoderma 216:48–61
Walker P, Green P (1976) Soil trends in two valley fill sequences. Soil Res 14:291–303
Webster R (1973) Automatic soil-boundary location from transect data. J Int Assoc Math Geol 5:27–37
Webster R (1978) Mathematical treatment of soil information. Transactions of the 11th International Congress of Soil Science, pp 161–190
Weindorf DC, Zhu Y, Haggard B, Lofton J, Chakraborty S, Bakr N, Zhang W, Weindorf WC, Legoria M (2012) Enhanced pedon horizonation using portable X-ray fluorescence spectrometry. Soil Sci Soc Am J 76:522–531
Wetselaar R (1962) Nitrate distribution in tropical soils. Plant Soil 16:19–31